Genome-wide Identification of Long Non-coding RNAs and Their Potential Functions in Poplar Growth and Phenylalanine Biosynthesis

Lei Zhang
Chinese Academy of Forestry
Xiaolan Ge
Chinese Academy of Forestry
Jiujun Du
Chinese Academy of Forestry
Jianjun Hu (hujj@caf.ac.cn)
Chinese Academy of Forestry

Research Article

Keywords: LncRNA-mRNA, poplar, phenylalanine biosynthesis, xylem, hormone

Posted Date: April 1st, 2021

DOI: https://doi.org/10.21203/rs.3.rs-363321/v1

Version of Record: A version of this preprint was published at Frontiers in Genetics on November 15th, 2021. See the published version at https://doi.org/10.3389/fgene.2021.762678.

Abstract

Background: Long non-coding RNAs (lncRNAs) represent a class of riboregulators that either directly act in long form or are processed into shorter microRNAs (miRNAs) and small interfering RNAs. Poplar is an important bioenergy tree species, lncRNAs play important roles in various biological regulatory processes, and its expression pattern is more tissue-specific than mRNA.

Results: In this study, *P. deltoides* 'Danhong' (Pd) and *P. simonii* 'Tongliao1' (Ps) with different growth rates and wood quality were used as experimental materials, and the transcriptomes of their shoot apical meristem, xylem, and phloem were sequenced. Furthermore, high-throughput RNA sequencing analysis revealed that the expression patterns of genes and lncRNAs are different between the two genotypes. 6, 355 lncRNAs were identified. Based on targets prediction, lncRNAs and target genes involved in ADP binding, oxidoreductase activity, phenylpropanoid biosynthesis, and cyanoamino acid metabolism. TCONS_00128372, TCONS_00079190, and TCONS_00174042 co-expressed with transcription factors and structural genes of lignin and flavonoid pathways. In addition, we found the potential target lncRNAs of miRNA.

Conclusion: This result provides basic evidence for a better understanding of the regulatory role of lncRNAs in regulating phenylalanine molecular pathways and wood formation.

Introduction

Plants are unique in their ability to continuously produce new organs throughout their life cycles. The process of continuous organogenesis depends on the activity of pluripotent cells [1]. In trees, this mainly refers to the shoot apical meristem (SAM), which regulates the height of plant growth, and the cambium, which affects radial growth. The SAM generates leaves, stems, and floral organs throughout the lifespan of higher plants [1, 2]. The cambium differentiated into xylem and phloem, determined cell types and cell layers in the secondary xylem [3]. These complex processes are easily regulated by plant hormones, transcription factors (TFs), miRNAs and lncRNAs [1, 4].

Populus, the important ecological protection and energy trees in China, the growth rate determines the economic benefit and the output of biomass energy. Aigeiros There are significant differences in the growth rate of *P. deltoides* 'Danhong' and *P. simonii* 'Tongliao1'. *P. deltoides* 'Danhong' is the American black poplar with fast growth and insect resistance [5]. *P. simonii* is a native tree species in northern China, although the growth rate is slow, it is resistant to cold and drought [6].

LncRNAs are non-coding transcripts longer than 200 nucleotides (nts), including intergenic, intronic, sense, and antisense types [7]. Compared with protein-coding genes (PCgenes), most lncRNAs are less conserved between species, low expression levels and stronger tissue-specific expression patterns [8–10]. LncRNAs can regulate gene expression at transcriptional, post-transcriptional and epigenetic levels, and play an important role in genomic imprinting, chromatin remodeling, transcriptional activation, transcriptional interference and cell cycle [11, 12]. With the continuous development of re-sequencing

technology, lncRNAs of more and more species have been identified. They are widely involved in embryo development, seed formation, flower development, secondary growth of wood, and abiotic stress response [8, 9, 13–15]. For example, lncRNAs play potential regulatory role in endosperm and embryo development of castor bean [9]. COOLAIR and COLDAIR play the important role in regulating vernalization in Arabidopsis [16]. *FLINC* lncRNA participated in ambient temperature-mediated flowering time of Arabidopsis [15]. LncRNAs influence the formation of tension wood by regulating *ARF*s in *Catalpa bungei* [17]. LncRNAs are widely involved in the secondary growth, GA response, heat tolerance, low nitrogen stress and other life processes of poplar [18–21].

In order to provide theoretical basis for breeding new germplasm with fast growing, we selected *P. deltoides* 'Danhong' and *P. simonii* 'Tongliao1' as experimental materials, and identified the important lncRNAs that may be involved in growth regulation by sequencing. In this study, the sequencing of long non-coding RNA libraries constructed from SAM and developing xylem of *P. deltoides* 'Danhong' and *P. simonii* 'Tongliao1' was done. The identification of lncRNAs was analyzed in reference to *P. tricorcarpa* genome. We identified a total of 6, 355 lncRNAs of which 2,455 were sense_overlapping lncRNAs, 2,005 were lincRNA, and 1897 were antisense lncRNAs. The functional prediction of lncRNAs and their expressions as involved in wood development were examined. We investigated putative functional lncRNA candidates (TCONS_00128372, TCONS_00079190, and TCONS_00174042) by differential expression analysis and co-expression network construction during SAM and xylem development. The important miRNAs-lncRNA pairs in phenylalanine biosynthesis and hormones transduction were identified.

Results

Differences in growth and wood properties between Pd and Ps

Wood is the secondary xylem of trees, mainly composed of cellulose, hemicellulose and lignin. All xylem cell types first undergo secondary cell wall (SCW) thickening and undergo programmed cell death [22, 23]. The plant height and ground diameter of annual Pd were significantly higher than that of Ps (**Fig. 1a and b**). Further material property determination found that the content of the three major elements of Pd is higher (**Fig. 1c-i**). SAM is an important regulatory site of plant height growth, phloem and developing xylem are important parts of plant radial growth. The anatomical structure showed that Pd had obvious shoot apex growth point (central zone), while Ps is not obvious (**Fig. 1j**). In addition, Pd exhibited wider phloem fiber and cambium, and larger vessel area and proportion, which may be beneficial to transports nutrient (**Fig. 1k**). The small basic density of Pd may be related to the large area occupied by the vessels (**Fig. 1l**).

Identification of lncRNAs from SAM, phloem, and developing xylem RNA-seq datasets

As an important fast-growing tree species, it is very important to understand the molecular pathways of growth and development of poplar. After trimming adapters and removing low quality and contaminated reads, in total, 246.24 Gb clean data was obtained from 18 libraries, with an average Q30 of 93.00%

(Additional file 6: Table S1). Finally, we identified 6, 355 lncRNAs with protections of 2,455 sense_overlapping lncRNAs, 2,005 of lincRNA, 1897 of antisense lncRNAs (Additional file 6: Table S2).

In order to characterize the characteristics of these lncRNAs, we evaluated the distribution of chromosome location, transcript length, exon number and expression level of lncRNAs. In general, lincRNA, sense_overlapping and antisense LncRNAs were evenly distributed on 19 chromosomes, although they had different emphases (**Fig. 2a**).The average length of lncRNAs was 990 bp and about 63.4% contained two exons (**Fig. 2b and c**). Antisense lncRNAs ranged in length from 201 to 9830 bp and average was 940 bp. LincRNAs ranged between 201and 4734 bp (average=783 bp). And average length of sense_overlapping lncRNAs is 1197 bp. The GC content of antisense lncRNA was 41.36%, which was significantly higher than that of lincRNAs and sense_overlapping lncRNAs (**Fig. 2d**). For expression levels, the lncRNAs expression levels were different and showed fewer average counts (FPKM=4.44) than the coding transcripts (FPKM=18.96) (**Fig. 2e and f**).

A principal component analysis (PCA) plot of the whole data set revealed a sequential order of the different samples. The results showed that SAM, xylem and phloem of the two species were clustered into one group, and the similarity between the two tissues was greater than that between genotypes (**Fig. 3a**).

Differentially expressed anaylsis between Pd and Ps

In order to further analyze whether these genes were differentially expressed between the two genotypes and different tissues, nine comparative combinations were carried out. Finally, 3, 573 differentially expressed (DE) lncRNAs and 27, 582 DEmRNAs were obtained. among them, the DElncRNAs of Pd_S vs. Ps_S is 1957 (**Fig. 3b and c,** Additional file 1:Figure S1). DEmRNAs participate in molecular functions such as “ADP binding” and “catalytic activity” (Additional file 1:Figure S1C).There are 980 DElncRNAs in two genotypes of the corresponding tissue comparison combination (Pd_ X vs. Ps_ X, Pd_ P vs. Ps_ P and Pd_ S vs. Ps_ S) (**Fig. 3d**). There are 322, 333 and 420 specifically expressed lncRNAs in SAM, xylem and phloem, respectively. Since lncRNAs play important roles in regulating gene expression, identification and analysis of their target genes may help us to explore their potential functions. Computational prediction identified a set of 12, 875 mRNAs corresponding to 8, 931 lncRNA–target pairs, including 6,565 colocation-regulated mRNAs for 3,551 lncRNAs and 7, 421 coexpression- regulated mRNAs for 3,285 lncRNAs.

To further analyze the function of these lncRNAs, we performed GO and KEGG analysis on their target genes. The colocation target genes of DElncRNAs were mainly enriched in 60 GO terms such as “ADP binding” and “nucleoside binding” (Additional file 2: Figure S2). Some target genes were enriched in photosynthesis pathway, including 39 lncRNAs and 68 mRNAs. And TCONS_00135489 showed the same trend as its target, and the expression level of related genes were high in SAM (Additional file 3: Figure S3).

The coexpression genes of Pd_ X vs. Ps_ X, Pd_ P vs. Ps_ P, and Pd_ S vs. Ps_ S were mainly related to “ADP binding”, “heme binding” and other biological functions (**Fig. 4a**). And they significantly enriched in the “phenylpropanoid biosynthesis” and “cyanoamino acid metabolism” pathway (**Fig. 4b**). These possible target genes provide new insight into the role of lncRNAs in poplar development.

Regulation of lncRNAs and transcription factors in the phenylpropanoid biosynthesis

Based on the predicted GO conditions of growth differential lncRNAs and the pathways associated with target genes, we speculated that lncRNAs might play an important role in phenylalanine biosynthesis in poplars. Phenylpropanoids are a group of plant secondary metabolites derived from phenylalanine, which has a variety of structural and signal molecular functions [24]. It is the starting compounds for biosynthesis of lignin, flavonoids, anthocyanins and so on, serves as the core mediators of crosstalk between developmental and defenserelated pathways [25]. Further analysis co-expression network of these lncRNAs and lignin, flavonoid biosynthesis, found that TCONS_00128372, incRNA, located in Chr12 and interact with *MYB46*, SECONDARY WALL- ASSOCIATED NAC DOMAIN2 (*SND2*), cinnamate-4-hydroxylase (*C4H*), caffeoyl-CoA 3-O-methyltransferase (*CcoAMT*), and laccase (*LAC*). And sense_overlapping lncRNA TCONS_00079190 co-expressed with *MYB83*, *MYB46*, NAC SECONDARY WALL THICKENING PROMOTIBNG FACTOR1 (*NST1*), and *LAC* (**Fig. 5a**). TCONS_00174042, TCONS_00101258, and TCONS_00136338 regulated the structural genes of flavonoid biosynthesis. TCONS_00174042 and TCONS_00101258 co-expressed with *MYB3*chalcone and stilbene synthase(*CHS*), leucoanthocyanidin reductase (*LAR*), leucoanthocyanidin dioxygenase (*LDOX*), and naringenin 3- dioxygenase (*F3H*). In addition, TCONS_00136338 can coexpress with *LDOX*, *CHS*, *UFGT*, *LAR*, and dihydroflavonol 4-reductase (*DFR*) (**Fig. 5b**). Lignin related lncRNAs and structural genes were highly expressed in xylem of Pd and Ps, while flavonoid related genes were highly expressed in SAM (Additional file 4: Figure S4).

LncRNAs involved in the plant hormone biosynthesis signal transduction pathway

Hormones, such as auxin, cytokinin, and gibberellin, play an important role in primay and secondary growth [26, 27]. In order to further analyze the relationship between lncRNA and plant hormones, we constructed a co-expression network including auxin, cytokinin, and gibberellin related PCgenes and their regulatory lncRNAs (**Fig. 6a**). TCONS_00134627 could be co expressed with *GA2OX8* (Potri.011G134000), *GASA10* (Potri.009G092600), and *SAUR94* (Potri.009G127300). The expression levels of DEGs and DElncRNAs related to auxin, cytokinin and gibberellin biosynthesis were shown in the heatmap (**Fig. 6b**).

miRNA involved in hormones and phenylalanine pathway

miRNAs, a major class of small RNAs with 20–24 nucleotides, create various aspects of plant development and stress responses through post transcriptionally regulation gene expression [28]. A total of 658 miRNA-lncRNA pairs consisting of 188 miRNAs and 200 lncRNAs were identified, including 19 plant hormone related pairs and 28 phenylalanine related pairs (Additional file 6: Table S3). TCONS_00066905, hormone related lncRNA, was predicted to be a target mimic of miR396a and

miR396b. In addition, phenylalanine related TCONS_00023606 and TCONS_ 00093325 is the target mimic of flavonoid related regulatory genes miR156h and miR828a (**Fig. 7a**). miR396-GRFs is an important regulatory module of plant growth and development. We found that 12 GRFs were differentially expressed and highly expressed in SAM of Pd, which may be an important reason for the rapid growth of Pd (**Fig. 7b**).

Validation of lncRNA and gene expression by qRT-PCR

To examine whether these differentially expressed lncRNAs had a role in xylem development and hormone signal transduction, related lncRNAs and mRNAs were selected based on their expression levels in RNA-seq. The results proved the reliability of transcriptome data (Additional file 5: **Figure S5**).

Discussion

Poplar is an important bioenergy in the world. Its growth rate and wood quality determine its economic value. With the development of RNA-seq technology, genome-wide mapping has been proved to be a powerful tool for studying primary and secondary growth of poplar. In this study, lncRNAs of woody plants was comprehensively analyzed to study the growth and development of woody plants and the regulation of wood quality. The transcriptomics of Pd and Ps were studied to identify lncRNA and mRNA related to growth and wood development. We identified 6, 355 lncRNAs, including 3, 573 DElncRNAs and 27, 582 DEGs. lncRNAs in Pd and Ps show similar characteristics with other species [19]. It is characterized by high tissue specificity and short length. The length of lncRNAs was about 991 bp, and the cis- and trans- effects were recognized. In this study, we identified a large number of trans regulatory networks, mainly acting on the phenylalanine pathway. These differentially expressed genes may be an important reason for the differences in growth rate and wood quality. There were significant differences in xylem, and the absence of SAM central region may result in slow growth of Ps.

The biosynthesis of secondary cell wall (SCW) in woody plants is highly related to the transformation and production of biofuels and biological products. It is regulated by microRNA, *MYB*, *NAC* and *WRKY* in SCW complex regulatory network [4]. As an important support of SCW, lignin determines the conversion efficiency of poplar as biomass energy. In previous studies, lncRNAs participates in the lignin biosynthesis of poplar with TFs and miRNAs [29, 30]. Also in our research, we found that 75 lncRNAs, including TCONS_00079190, TCONS_00128372, and TCONS_00007135, can be directly co-expressed with *MYB*s, *VND*s and lignin structural genes (**Fig. 5a**). Flavonoids and lignin are the metabolic pathways of phenylalanine metabolism, and there are some common structural genes. At the same time, flavonoids are important compounds for plants to respond to biological and abiotic stresses. lncRNAs involved in regulating the anthocyanin biosynthetic pathways in strawberry, buckthorn and apple fruit [32–34]. We identified a large number of lncRNAs co expressed with structural genes of flavonoid pathway such as *CHS* and *DFR*（**Fig. 5b**）. The insertion of five cisgenes encoding gibberellin metabolism or signal proteins affects plant growth [31]. The auxin-mediated Aux/IAA-ARF-HB signal cascade regulates the development of the secondary xylem of poplar [26]. And it was found that a large number of auxin and gibberellin

related lncRNA-mRNA coexpression networks were identified (**Fig. 6**), which was similar with endogenous hormone regulation in secondary xylem and during tension wood formation in *Catalpa bungei* [17]. Therefore, lncRNAs were widely involved in the lignin, flavonoid metabolism and plant growth of Pd and Ps and affects their differences.

Post-transcriptional regulation is an important process affecting gene expression and plant development [28, 35]. miR156 and miR828 are involved in the biosynthesis of flavonoids and anthocyanins by regulating *MYB*s in many species [36–38]. We identified TCONS_00023606 and TCONS_00093325 as the target gene of miRNA156 and miR828, so they may indirectly participate in the transcriptional regulation of flavonoids through this pathway (Fig. 7, Additional file 6: Table S3). miR396, *GRF*s and GRF-INTERACTING FACTORS (*GIF*s) has been proven to control the growth of multiple tissues and organs of multiple species [39, 40]. *GRF*s are important regulators of SAM, which are the starting sites of leaf and stem development [41]. The high expression of *GRFs* in Pd_ S may be an important reason for the rapid growth of Pd. lncRNAs-miRNAs-TFs-mRNAs play an important role in regulating the growth of poplars. Therefore, the differences in the growth rate and wood quality of the two poplars may be caused by the joint regulation of these factors, which requires our follow-up further functional verification.

Conclusions

In this study, we compared the differences in SAM and xylem of Pd and Ps with significant differences in growth speed and wood properties. In total, 3, 573 DElncRNAs and 27, 582 DEGs were detected during plant growth. In addition, 1240 lncRNA-mRNA interaction pairs were predicted to be involved in flavonoids and lignin biosynthesis. Moreover, the TCONS_00023606 was a precursor of miR156, which targets the *SPL* module of genes to enable flavonoids. This study will provide a basis for subsequent studies on the molecular biology of the wood formation and plant growth.

Methods

Plant materials

One-year-old *P. deltoides* 'Danhong' (Pd) and *P. simonii* 'Tongliao1' (Ps) cultivated in the experimental field of Chinese Academy of Forestry, Beijing, China (116.256°E, 40.007°N). We collected shoot apical meristem (SAM, Pd_S and Ps_S), and scraped phloem (inside of the bark, Pd_P and Ps_P) and developing xylem (newly formed xylem cells about 2-3mm, Pd_X and Ps_X) from Pd and Ps at diameter breast height (DBH) during the fast-growing period (July 20, 2019). Each sample had three biological replicates. The samples used for RNA extraction were frozen immediately in liquid nitrogen, and stored at −80 °C. Cuneiform blocks, including phloem, cambium, and xylem, at DBH for histological analysis were fixed in formalin: glacial acetic acid: 70% ethanol (5:5:90 vol.; FAA) solution under a vacuum for at least 24 h.

Histological analysis

Stem pieces were embedded with Spurr resin as described by Zhang [22].Cross section of 4-μm thick was obtained from stem by Leica M205FA. SAM sections 40μm thick were obtained using a rotary microtome (Leica VT1200S, Wetzlar, Germany). Sections were stained by 0.05% toluidine blue O (TBO) and were examined with microscope (Zeiss).

Wood properties determination

In order to understand the difference of wood properties between Pd and Ps, we measured the plant height and ground diameter, and collected the stems to measure the wood properties including basic density, fiber length, fiber width, microfibril angle, cellulose, holocellulose and lignin content in December 2019. The basic density was determined by drainage method. A 10 cm high wood segment was cut from the base of the trunk to without bark and pith. It is softened by heating in 30% nitric acid and a small amount of potassium chlorate and converted into wood pulp by forced oscillation. The length and width of the fiber were measured 50 times by Shyygx Measure 2.0. Wood flour (40-60 mesh) from 5 cm basal stem segment was used to determine chemical composition. The content of holocellulose and lignin was calculated according to Chinese standard GB/T 2677.10-1995 and GB/T 2677.8-1994, respectively. To evaluate the content of cellulose, specimens were extracted with a mixed solvent of nitric acid and ethanol (v/v = 1/1) [42]. Three replicates were performed for each variety.

Total RNA isolation, library construction, and Illumina transcriptome sequencing

Total RNA was isolated from the 18 samples (SAM, phloem and developing xylem) using RNAprep Pure Plant Plus Kit (TIANGEN, China). An index of the reference genome (*P. trichocarpa* 3.0) was built using HISA T2 [43]. StringTie was used to calculate FPKMs of both lncRNAs and coding genes in each sample [44].

LncRNA identification

We used four filtration steps to identify lncRNAs from transcriptome assembly: (1) The transcripts with exon number ≥ 2 and length ≥ 200bp were selected. (2) Use CuffCompare software to screen out transcripts that overlap with the database annotation exon field. (3) Use evaluation of Coding Potential Calculator (CPC) [45], Coding-Potential Assessment Tool (CPAT) [46], and Coding-Non-Coding Index(CNCI) [47] to screen whether there is coding potential. (4) Referred to HGNC (The Hugo Gene Nomenclature Committee) to name the Novel_lncRNA of this analysis.

Target gene prediction

Two methods were used to predict lncRNA target genes. *cis* target genes were predicted according to the location relationship between lncRNA and mRNA, and the screening range was within 100kb. Co-expression related target genes were predicted according to the expression correlation between lncRNA and mRNA, the screening condition is that the correlation coefficient is greater than 0.95. The mRNA–lncRNA regulatory network was further modeled visualized by Cytoscape 3.8 [48].

In order to identify lncRNAs that may be used as precursors of miRNAs, we compared the published miRNAs of *P. trichocarpa* in miRBase (http://www.mirbase.org/search.shtml) with lncRNAs. The secondary structures of lncRNAs and miRNAs were predicted with RNAfold WebServer (http://rna.tbi.univie.ac.at/cgi-bin/RNAWebSuite/RNAfold.cgi). LncRNAs as targets of miRNAs were predicted by the Novomagic, a free online platform for data analysis (https://magic.novogene.com).

DElncRNA and Functional Analysis

To identify the differential expression lncRNAs and mRNAs between the Pd and Ps, we performed pair-wise comparisons (Pd_S vs. Ps_S, Pd_P vs. Ps_P, Pd_X vs. Ps_X, Pd_S vs. Pd_P, Pd_S vs. Pd_X, Pd_P vs. Pd_X, Ps_S vs. Ps_P, Ps_S vs. Ps_X, Ps_P vs. Ps_X) by DESeq R package with q-value < 0.05 [49]. Finally, those putative cis- and coexpression-targets of lncRNAs were analysed using gene ontology (GO) [50, 51]. And KEGG (Kyoto Encyclopedia of Genes and Genomes) enrichment of DE genes were performed based on corrected P-value < 0.05.

Quantitative real-time (qRT)-PCR and correlation analysis of expression trends

We selected 3 DELs and 3 DEGs from the results of the transcriptional analysis and confirmed them by qRT-PCR. *PtrActin* was used as internal reference gene (Additional file 6: **Table S4**). The relative expression levels of the genes were calculated using the $2^{-\Delta\Delta CT}$ method [52], and the data are presented as the mean ± SD from three independent biological replicates.

Declarations

Acknowledgments

We would like to thank the reviewers and editors for their careful reading and helpful comments on this manuscript.

Authors' contributions

LZ and JH conceived and designed the project. LZ, XG and JD participated in the experiments and data analysis. LZ drafted the manuscript. LZ and JH modified manuscript. All authors read and approved the final manuscript.

Funding

This study was supported by the National Natural Science Foundation (32071797, 31570669) and the National Key Programon Transgenic Research (2018ZX08020002).

Availability of data and materials

All raw data from Illumina sequencing including lncRNAs and RNA-seq data have been submitted to the SRA database under the accession number PRJNA714425.

Ethics approval and consent to participate

Not applicable.

Consent for publication

Not applicable.

Competing interests

The authors declare that they have no competing interests.

Author details

References

1. Xue Z, Liu L, Zhang C. Regulation of shoot apical meristem and axillary meristem development in plants. Int J Mol Sci 2020. doi:10.3390/ijms21082917.
2. Ha CM, Jun JH, Fletcher JC. Shoot apical meristem form and function. Curr Top Dev Biol. 2010;91:103–40. doi:10.1016/S0070-2153(10)91004-1.
3. Ye Z-H, Zhong R. Molecular control of wood formation in trees. J Exp Bot. 2015;66:4119–31. doi:10.1093/jxb/erv081.
4. Zhang J, Xie M, Tuskan GA, Muchero W, Chen J-G. Recent advances in the transcriptional regulation of secondary cell wall biosynthesis in the woody plants. Front Plant Sci. 2018;9:1535. doi:10.3389/fpls.2018.01535.
5. Zhang C, Li S, Zhao Z, Hu J, Han Y. A new poplar variety *Populus deltoides* 'Danhong'. Scientia Silvae Sinicae. 2008:169. doi:10.11707/j.1001-7488.20080127.
6. Wei Z, Du Q, Zhang J, Li B, Zhang D. Genetic diversity and population structure in Chinese indigenous poplar (*Populus simonii*) populations Using Microsatellite Markers. Plant Molecular Biology Reporter. 2013;31:620–32. doi:10.1007/s11105-012-0527-2.
7. Ma L, Bajic VB, Zhang Z. On the classification of long non-coding RNAs. RNA Biol. 2013;10:925–33. doi:10.4161/rna.24604.
8. Zhou D, Du Q, Chen J, Wang Q, Zhang D. Identification and allelic dissection uncover roles of lncRNAs in secondary growth of *Populus tomentosa*. DNA Res. 2017;24:473–86. doi:10.1093/dnares/dsx018.
9. Xu W, Yang T, Wang B, Han B, Zhou H, Wang Y, et al. Differential expression networks and inheritance patterns of long non-coding RNAs in castor bean seeds. Plant J. 2018;95:324–40. doi:10.1111/tpj.13953.
10. Liu J, Jung C, Xu J, Wang H, Deng S, Bernad L, et al. Genome-wide analysis uncovers regulation of long intergenic noncoding RNAs in Arabidopsis. Plant Cell. 2012;24:4333–45. doi:10.1105/tpc.112.102855.

11. Wang H-LV, Chekanova JA. Long noncoding RNAs in plants. Adv Exp Med Biol. 2017;1008:133–54. doi:10.1007/978-981-10-5203-3_5.
12. Sun X, Zheng H, Sui N. Regulation mechanism of long non-coding RNA in plant response to stress. Biochem Biophys Res Commun. 2018;503:402–7. doi:10.1016/j.bbrc.2018.07.072.
13. Wu X, Shi T, Iqbal S, Zhang Y, Liu L, Gao Z. Genome-wide discovery and characterization of flower development related long non-coding RNAs in *Prunus mume*. BMC Plant Biol. 2019;19:64. doi:10.1186/s12870-019-1672-7.
14. Jiang H, Jia Z, Liu S, Zhao B, Li W, Jin B, Wang L. Identification and characterization of long non-coding RNAs involved in embryo development of *Ginkgo biloba*. Plant Signal Behav. 2019;14:1674606. doi:10.1080/15592324.2019.1674606.
15. Severing E, Faino L, Jamge S, Busscher M, Kuijer-Zhang Y, Bellinazzo F, et al. *Arabidopsis thaliana* ambient temperature responsive lncRNAs. BMC Plant Biol. 2018;18:145. doi:10.1186/s12870-018-1362-x.
16. Heo JB, Sung S. Vernalization-mediated epigenetic silencing by a long intronic noncoding RNA. Science. 2011;331:76–9. doi:10.1126/science.1197349.
17. Xiao Y, Yi F, Ling J, Yang G, Lu N, Jia Z, et al. Genome-wide analysis of lncRNA and mRNA expression and endogenous hormone regulation during tension wood formation in *Catalpa bungei*. BMC Genomics. 2020;21:609. doi:10.1186/s12864-020-07044-5.
18. Tian J, Song Y, Du Q, Yang X, Ci D, Chen J, et al. Population genomic analysis of gibberellin-responsive long non-coding RNAs in *Populus*. J Exp Bot. 2016;67:2467–82. doi:10.1093/jxb/erw057.
19. Ci D, Tian M, Song Y, Du Q, Quan M, Xuan A, et al. Indole-3-acetic acid has long-term effects on long non-coding RNA gene methylation and growth in *Populus tomentosa*. Mol Genet Genomics. 2019;294:1511–25. doi:10.1007/s00438-019-01593-5.
20. Chen M, Wang C, Bao H, Chen H, Wang Y. Genome-wide identification and characterization of novel lncRNAs in *Populus* under nitrogen deficiency. Mol Genet Genomics. 2016;291:1663–80. doi:10.1007/s00438-016-1210-3.
21. Song Y, Chen P, Liu P, Bu C, Zhang D. High-temperature-responsive poplar lncRNAs modulate target gene expression via RNA interference and act as RNA scaffolds to enhance heat tolerance. Int J Mol Sci 2020. doi:10.3390/ijms21186808.
22. Zhang L, Liu B, Zhang J, Hu J. Insights of molecular mechanism of xylem development in five black poplar cultivars. Front Plant Sci. 2020;11:620. doi:10.3389/fpls.2020.00620.
23. Zhong R, Ye Z-H. Secondary cell walls: biosynthesis, patterned deposition and transcriptional regulation. Plant Cell Physiol. 2015;56:195–214. doi:10.1093/pcp/pcu140.
24. Costa MA, Collins RE, Anterola AM, Cochrane FC, Davin LB, Lewis NG. An in silico assessment of gene function and organization of the phenylpropanoid pathway metabolic networks in *Arabidopsis thaliana* and limitations thereof. Phytochemistry. 2003;64:1097–112. doi:10.1016/S0031-9422(03)00517-X.

25. Alessandra L, Luca P, Adriano M. Differential gene expression in kernels and silks of maize lines with contrasting levels of ear rot resistance after Fusarium verticillioides infection. J Plant Physiol. 2010;167:1398–406. doi:10.1016/j.jplph.2010.05.015.
26. Xu C, Shen Y, He F, Fu X, Yu H, Lu W, et al. Auxin-mediated Aux/IAA-ARF-HB signaling cascade regulates secondary xylem development in *Populus*. New Phytol. 2019;222:752–67. doi:10.1111/nph.15658.
27. Nieminen K, Immanen J, Laxell M, Kauppinen L, Tarkowski P, Dolezal K, et al. Cytokinin signaling regulates cambial development in poplar. Proc Natl Acad Sci U S A. 2008;105:20032–7. doi:10.1073/pnas.0805617106.
28. Yu Y, Zhang Y, Chen X, Chen Y. Plant noncoding RNAs: hidden players in development and stress responses. Annu Rev Cell Dev Biol. 2019;35:407–31. doi:10.1146/annurev-cellbio-100818-125218.
29. Quan M, Du Q, Xiao L, Lu W, Wang L, Xie J, et al. Genetic architecture underlying the lignin biosynthesis pathway involves noncoding RNAs and transcription factors for growth and wood properties in Populus. Plant Biotechnol J. 2019;17:302–15. doi:10.1111/pbi.12978.
30. Zhang J, Tuskan GA, Tschaplinski TJ, Muchero W, Chen J-G. Transcriptional and post-transcriptional regulation of lignin biosynthesis pathway genes in *Populus*. Front Plant Sci. 2020;11:652. doi:10.3389/fpls.2020.00652.
31. Han KM, Dharmawardhana P, Arias RS, Ma C, Busov V, Strauss SH. Gibberellin-associated cisgenes modify growth, stature and wood properties in *Populus*. Plant Biotechnol J. 2011;9:162–78. doi:10.1111/j.1467-7652.2010.00537.x.
32. Yang T, Ma H, Zhang J, Wu T, Song T, Tian J, Yao Y. Systematic identification of long noncoding RNAs expressed during light-induced anthocyanin accumulation in apple fruit. Plant J. 2019;100:572–90. doi:10.1111/tpj.14470.
33. Lin Y, Jiang L, Chen Q, Li Y, Zhang Y, Luo Y, et al. Comparative transcriptome profiling analysis of red- and white-Fleshed strawberry (*Fragariaï ananassa*) provides new insight into the regulation of the anthocyanin pathway. Plant Cell Physiol. 2018;59:1844–59. doi:10.1093/pcp/pcy098.
34. Zhang G, Chen D, Zhang T, Duan A, Zhang J, He C. Transcriptomic and functional analyses unveil the role of long non-coding RNAs in anthocyanin biosynthesis during sea buckthorn fruit ripening. DNA Res. 2018;25:465–76. doi:10.1093/dnares/dsy017.
35. Li C, Zhang B. MicroRNAs in control of plant development. J. Cell. Physiol. 2016;231:303–13. doi:10.1002/jcp.25125.
36. Wang Y, Liu W, Wang X, Yang R, Wu Z, Wang H, et al. MiR156 regulates anthocyanin biosynthesis through SPL targets and other microRNAs in poplar. Hortic Res. 2020;7:118. doi:10.1038/s41438-020-00341-w.
37. Zhang B, Yang H-J, Yang Y-Z, Zhu Z-Z, Li Y-N, Qu D, Zhao Z-Y. mdm-miR828 Participates in the feedback loop to regulate anthocyanin accumulation in apple peel. Front Plant Sci. 2020;11:608109. doi:10.3389/fpls.2020.608109.

38. Tirumalai V, Swetha C, Nair A, Pandit A, Shivaprasad PV. miR828 and miR858 regulate VvMYB114 to promote anthocyanin and flavonol accumulation in grapes. J Exp Bot. 2019;70:4775–92. doi:10.1093/jxb/erz264.
39. Liebsch D, Palatnik JF. MicroRNA miR396, GRF transcription factors and GIF co-regulators: a conserved plant growth regulatory module with potential for breeding and biotechnology. Curr Opin Plant Biol. 2020;53:31–42. doi:10.1016/j.pbi.2019.09.008.
40. Debernardi JM, Mecchia MA, Vercruyssen L, Smaczniak C, Kaufmann K, Inze D, et al. Post-transcriptional control of GRF transcription factors by microRNA miR396 and GIF co-activator affects leaf size and longevity. Plant J. 2014;79:413–26. doi:10.1111/tpj.12567.
41. Wang J, Zhou H, Zhao Y, Sun P, Tang F, Song X, Lu M-Z. Characterization of poplar growth-regulating factors and analysis of their function in leaf size control. BMC Plant Biol. 2020;20:509. doi:10.1186/s12870-020-02699-4.
42. Zhan T, Lu J, Zhou X, Lu X. Representative volume element (RVE) and the prediction of mechanical properties of diffuse porous hardwood. Wood Science and Technology. 2015;49:147–57. doi:10.1007/s00226-014-0687-3.
43. Kim D, Langmead B, Salzberg SL. HISAT: a fast spliced aligner with low memory requirements. Nat Methods. 2015;12:357–60. doi:10.1038/nmeth.3317.
44. Pertea M, Pertea GM, Antonescu CM, Chang T-C, Mendell JT, Salzberg SL. StringTie enables improved reconstruction of a transcriptome from RNA-seq reads. Nat Biotechnol. 2015;33:290–5. doi:10.1038/nbt.3122.
45. Kong L, Zhang Y, Ye Z-Q, Liu X-Q, Zhao S-Q, Wei L, Gao G. CPC: assess the protein-coding potential of transcripts using sequence features and support vector machine. Nucleic Acids Res. 2007;35:W345-9. doi:10.1093/nar/gkm391.
46. Wang L, Park HJ, Dasari S, Wang S, Kocher J-P, Li W. CPAT: Coding-Potential Assessment Tool using an alignment-free logistic regression model. Nucleic Acids Res. 2013;41:e74. doi:10.1093/nar/gkt006.
47. Sun L, Luo H, Bu D, Zhao G, Yu K, Zhang C, et al. Utilizing sequence intrinsic composition to classify protein-coding and long non-coding transcripts. Nucleic Acids Res. 2013;41:e166. doi:10.1093/nar/gkt646.
48. Otasek D, Morris JH, Bouças J, Pico AR, Demchak B. Cytoscape Automation: empowering workflow-based network analysis. Genome Biology. 2019;20:185. doi:10.1186/s13059-019-1758-4.
49. Love M, Anders S, Huber W. Differential analysis of count data–the deseq2 package. Genome Biology. 2014;15.
50. Ashburner M, Ball CA, Blake JA, Botstein D, Butler H, Cherry JM, et al. Gene ontology: tool for the unification of biology. The Gene Ontology Consortium. Nat Genet. 2000;25:25–9. doi:10.1038/75556.
51. Conesa A, Götz S, García-Gómez JM, Terol J, Talón M, Robles M. Blast2GO: a universal tool for annotation, visualization and analysis in functional genomics research. Bioinformatics.

2005;21:3674–6. doi:10.1093/bioinformatics/bti610.

52. Livak KJ, Schmittgen TD. Analysis of relative gene expression data using real-time quantitative PCR and the 2(-Delta Delta C(T)) Method. Methods. 2001;25:402–8. doi:10.1006/meth.2001.1262.

Figures

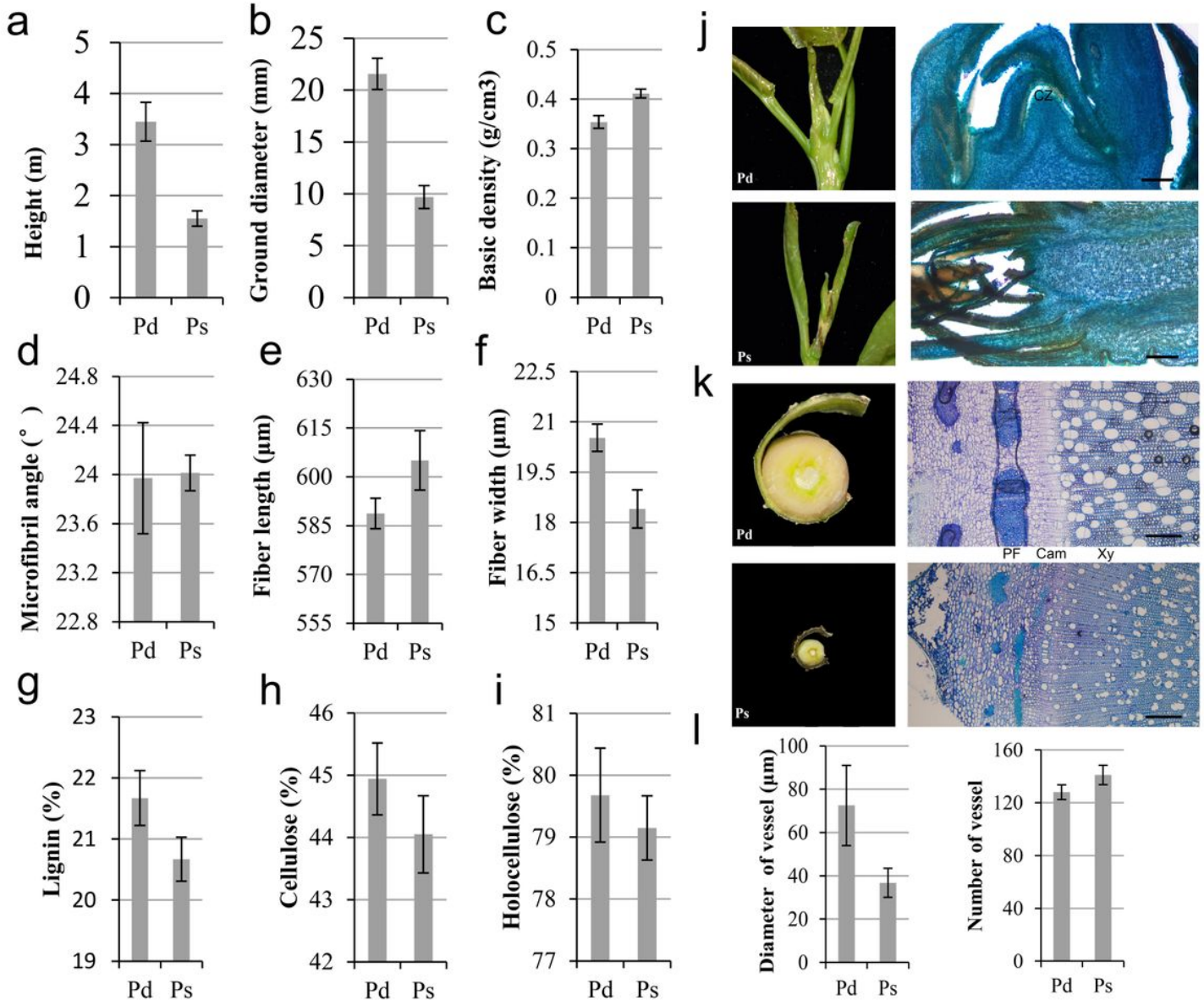

Figure 1

Phenotypic traits of P. deltoides ‘Danhong’ (Pd) and P. simonii ‘Tongliao1’ (Ps). Annual plant height (a), ground diameter (b), basic density (c), microfibril angle (d), fiber length (e), fiber width (f), lignin (g), cellulose (h), and holocellulose (i) content of Pd and Ps. j The shoot apical meristem (SAM) image and section of Pd and Ps. k Cross sections of phloem–xylem region from 1-year-old trees. Scale bars = 200μm. l Vessel size and number of vessel in the same area of Pd and Ps. CZ, central zone; PF, phloem fiber; Cam, cambium; Xy, xylem.

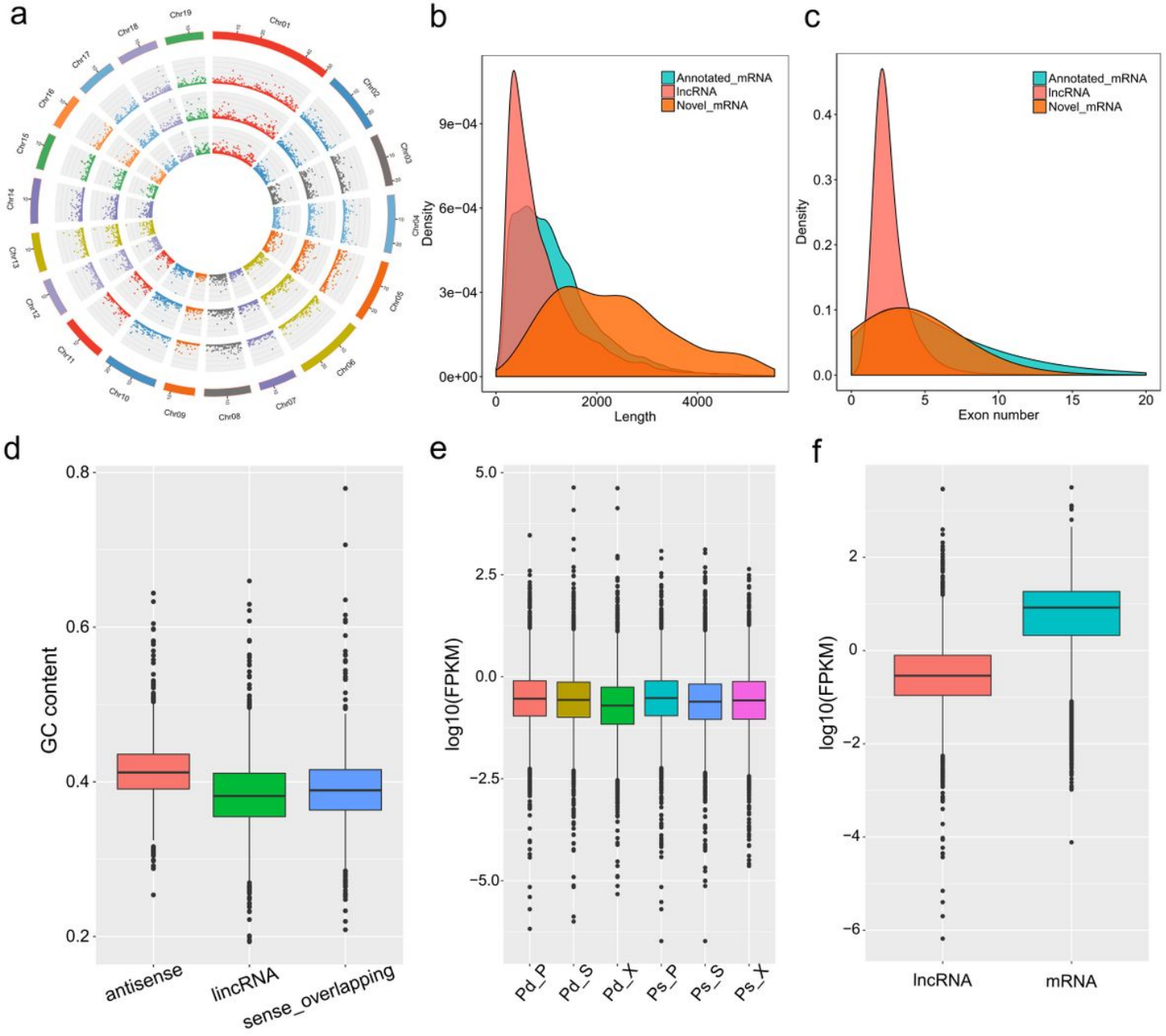

Figure 2

Characterization of cassava lncRNAs in Pd and Ps. a Distribution of lncRNAs along each chromosome for SAM, phloem, and xylem in Pd. Distributions of length density (b) and exon numbers (c) in mRNAs, novel mRNAs and novel lncRNAs. d The GC content of lncRNAs. e Boxplot of fragments per kilobase per million reads (FPKM) values. f The FPKM of mRNA and lncRNAs.

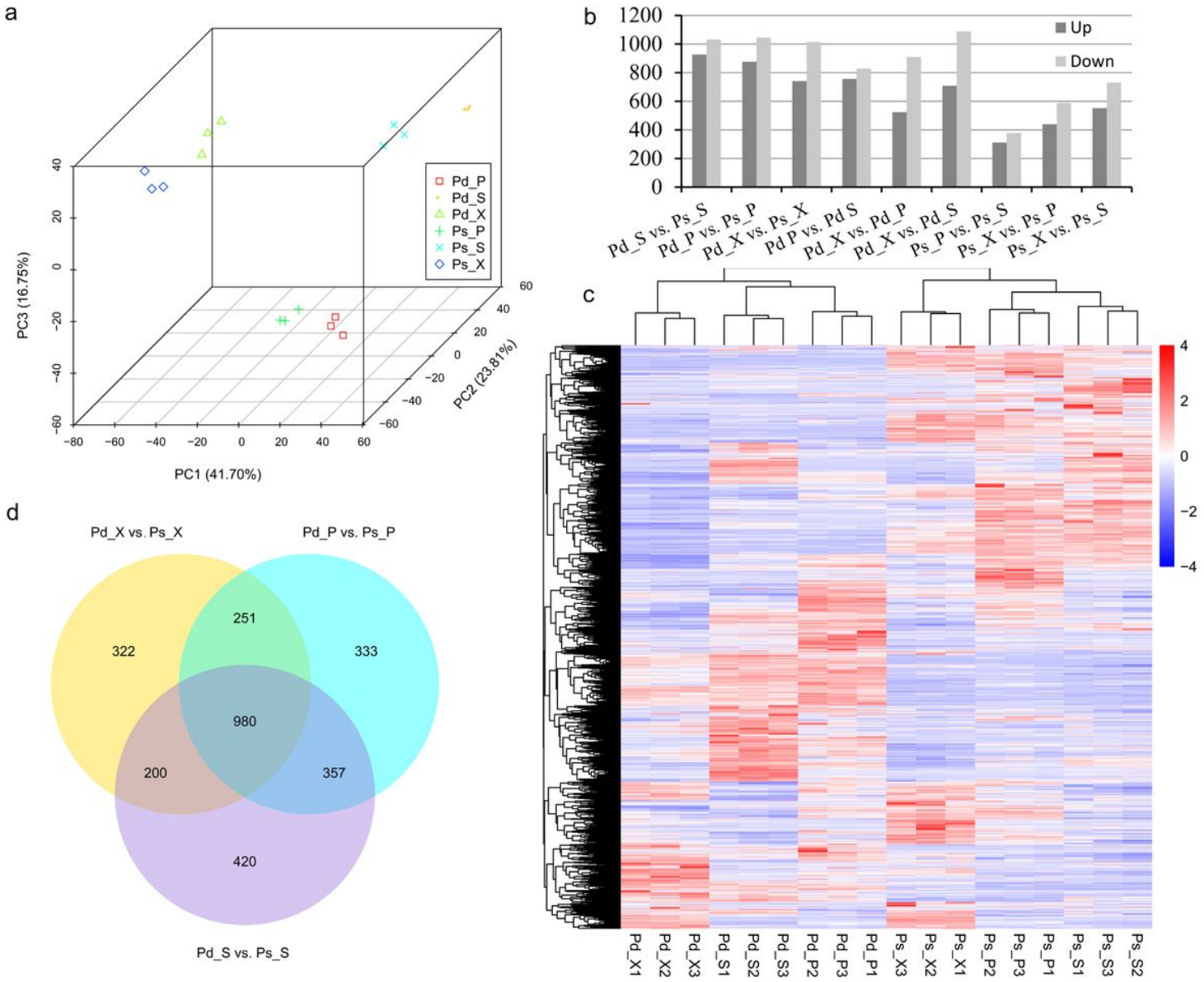

Figure 3

Differentially expressed (DE) lncRNAs identified in pair-wise comparison of 18 samples. a Principal component analysis (PCA) 3D of the expressed genes showing sample separation. b The number of DElncRNAs in different comparisons. b The heat map of DElncRNAs in the two genotypes. d Venn diagrams.

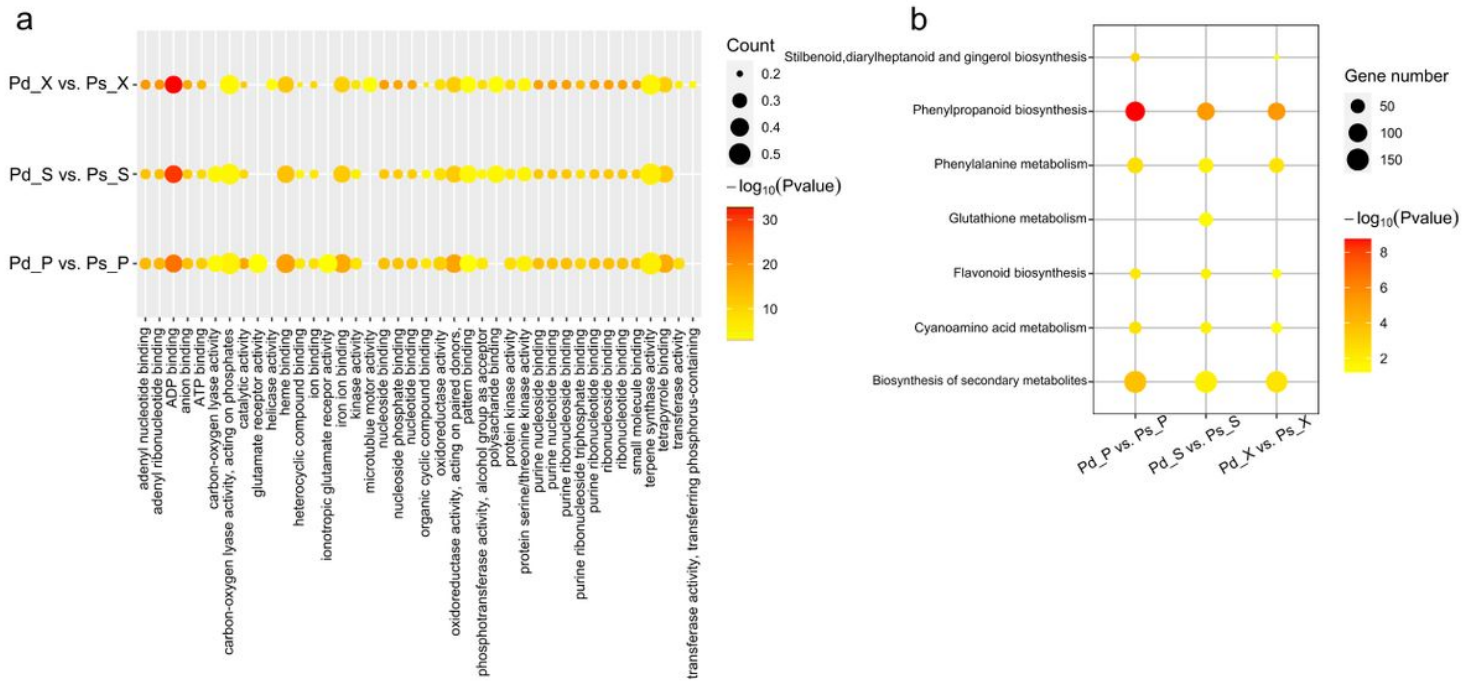

Figure 4

The co-expressiion mRNA of DElncRANs GO and KEGGs enrichment. a GO enrichment analysis of differentially expressed LncRNA-target genes. b KEGG enrichment analysis of differentially expressed LncRNA-target genes.

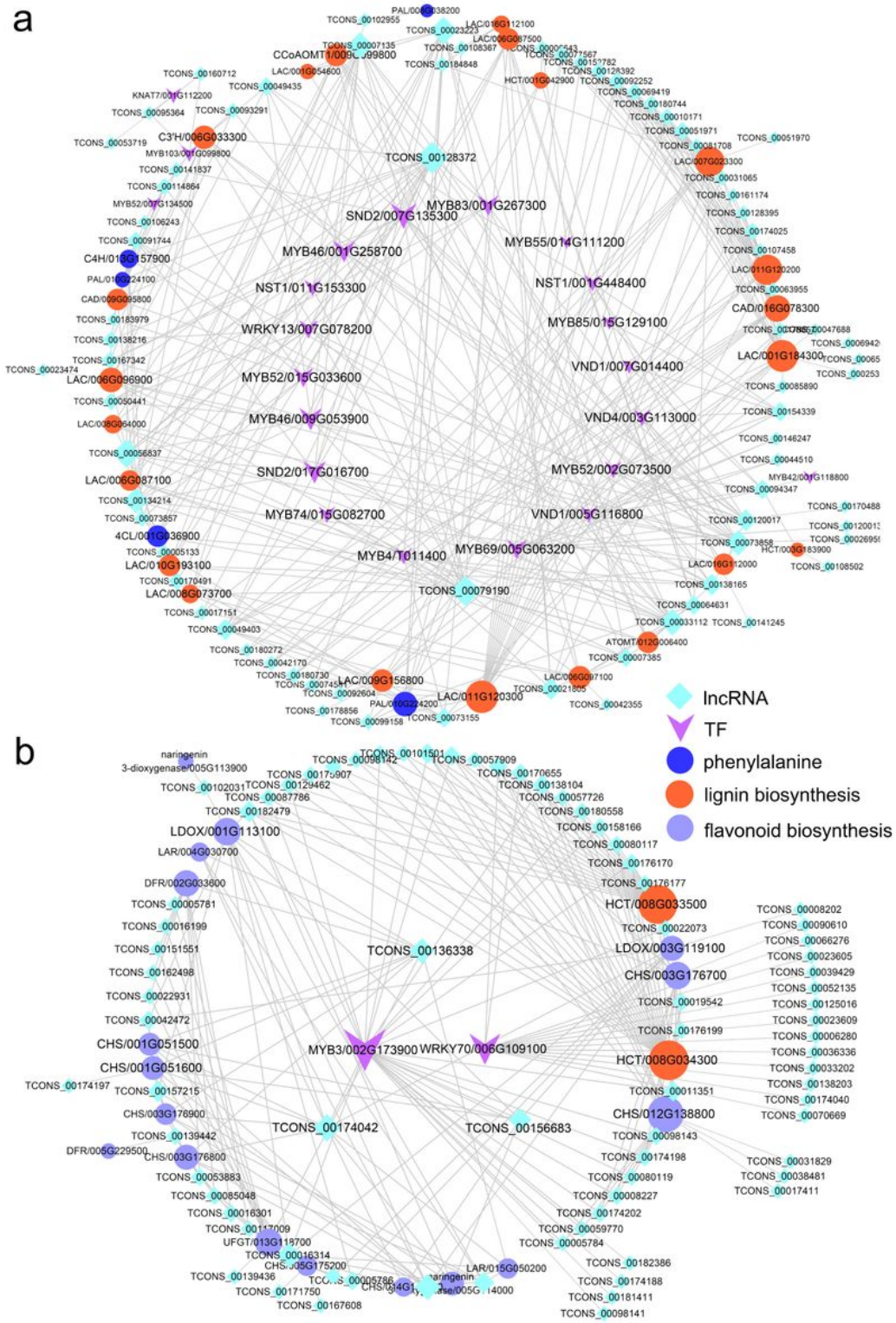

Figure 5

Interaction network diagrams. Interaction networks of differentially expressed lncRNAs, DEmRNAs and transcription factors (TFs) of phenylalanine biosynthesis, including lignin (a) and flavonoid (b) biosynthesises.

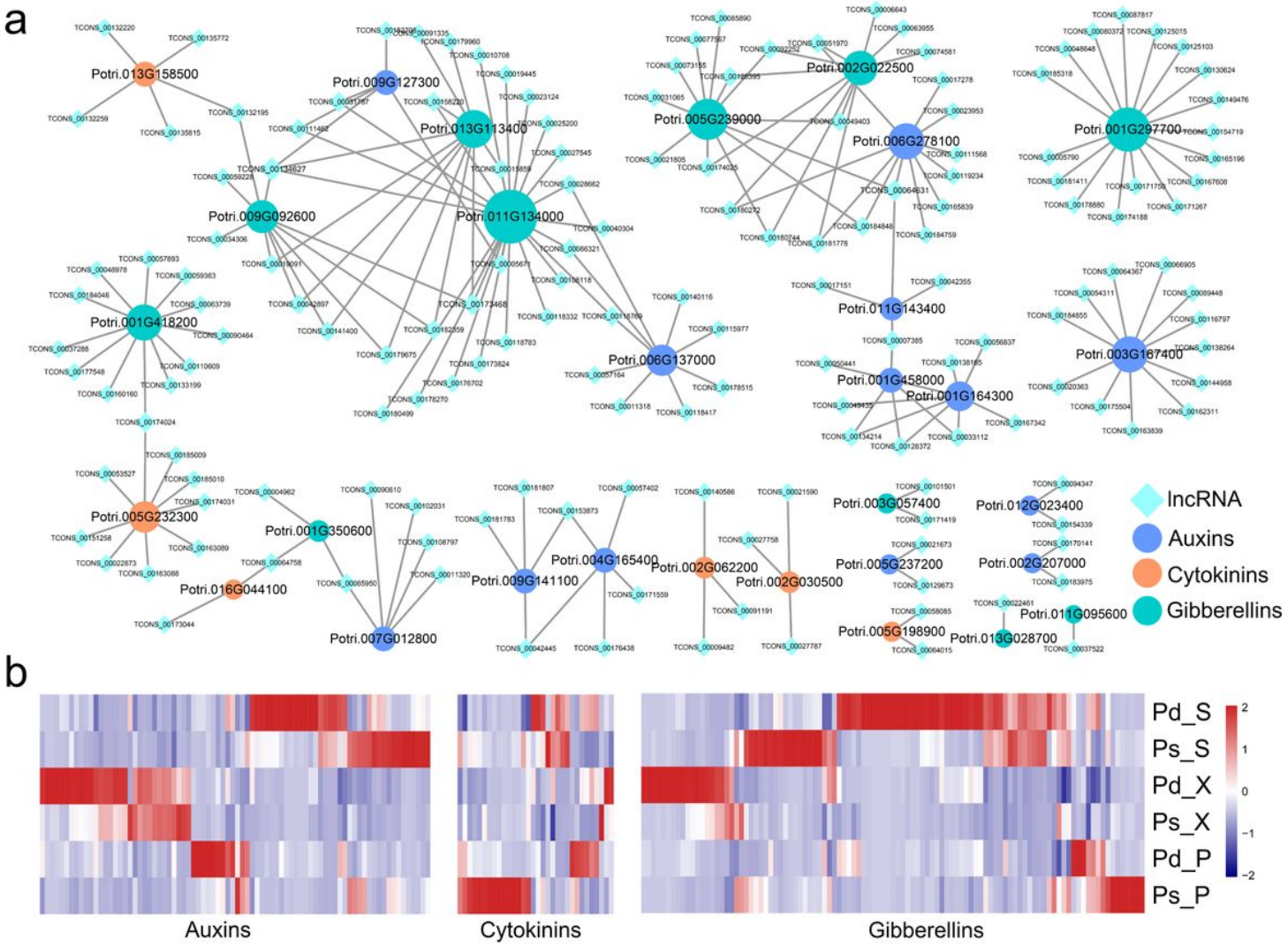

Figure 6

LncRNAs related to plant hormone biosynthesis and signal transduction. a Co-expression network of DElncRNAs and protein coding genes (PCgenes) involved in auxins, cytokinins, and gibberellins biosynthesis and signal transduction. b Expression of selected lncRNAs and their predicted co-expression target PCgenes involved in plant hormone biosynthesis signal transduction.

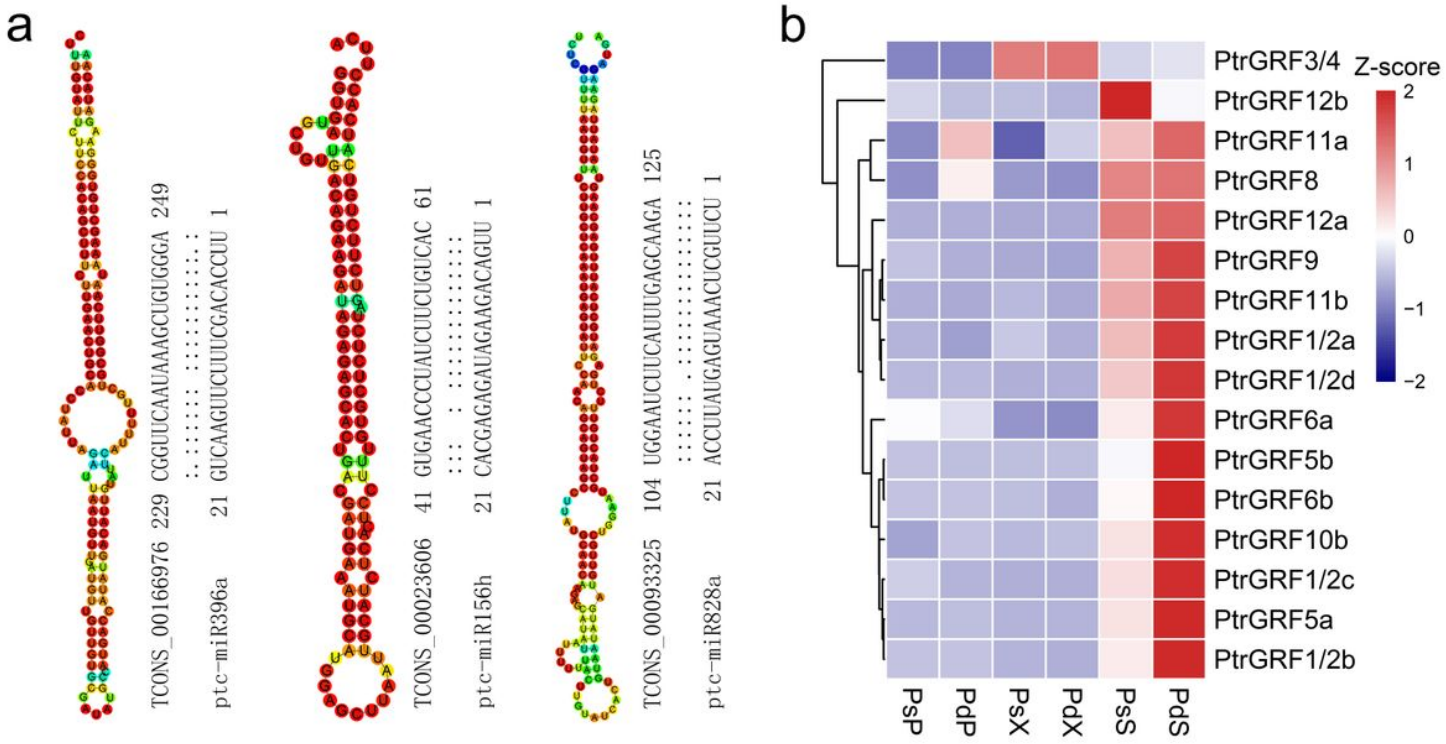

Figure 7

Expression analysis of related lncRNAs as potential targets or target mimics of miRNAs. a Sequence alignment of miRNAs and their potential target lncRNAs. b The expression patterns of differentially expressed GRFs, the target genes of miR396, in the two species.

Supplementary Files

This is a list of supplementary files associated with this preprint. Click to download.

- Additionalfile1FigureS1.jpg
- Additionalfile2FigureS2.jpg
- Additionalfile3FigureS3.jpg
- Additionalfile4FigureS4.jpg
- Additionalfile5FigureS5.jpg
- Additionalfile6TableS14.xlsx